

The efficiency of overshoot and undershot waterwheels

M Denny

5114 Sandgate Road, Victoria, BC, V9C 3Z2, Canada

E-mail: markandjane@shaw.ca

Received 5 September 2003

Published 2 December 2003

Online at stacks.iop.org/EJP/25/193 (DOI: 10.1088/0143-0807/25/2/006)

Abstract

The waterwheel evolved over two millennia to become an efficient machine. We analyse the physics of waterwheels, and construct simple models that show why the two most important types had very different efficiencies. Our analysis reveals the important design parameters, and captures the essential features of our oldest mechanical power source.

1. Introduction and history

Physicists commonly adopt the waterwheel as an analogy for other physical systems; the flow of water may represent the flow of electricity, or steam, with the capacity to do work. More recently it has been adopted as a representation of the Lorenz equations, so that for certain regions of the parameter space, this strange waterwheel behaves chaotically¹ [1]. In this paper we shall consider this oldest of machines not as an analogy, nor as a representation of some other physical system, but shall instead investigate the historically important waterwheel designs, to see why they developed the way they did. In particular, we shall calculate the efficiencies of several types of waterwheel. This is an instructive application of Newton's laws, energy transfer, power, torque, and elementary fluid mechanics to a familiar and important machine, which will shed light upon the design features that exercised the minds of many well known and unknown scientists and engineers over the ages.

The waterwheel has evolved steadily since it was introduced 2000 years ago, to pump water and mill grain. From the rather scant records of classical antiquity it is not clear where it originated; it is clear that it spread rapidly and is described by Roman, Greek and Chinese sources. These early machines (the 'Greek' or 'Norse' mill) had horizontal wheels, i.e. with vertical shafts, since these are simplest and required no gearing to transmit power to the millstone [2, 3]. There is good evidence that the familiar vertical waterwheel (with horizontal axle) developed within the Roman Empire [4] and spread out rapidly from there. The *undershot* waterwheel (so-called because the water passes underneath the axle) is described by Vitruvius

¹ A chaotic waterwheel has been built at the Fachhochschule Brugg-Windisch (Switzerland). The chaotic character of this device is described in the website <http://people.web.psi.ch/gassmann/waterwheel/WaterwheelLab.html>, where an interactive simulation is available.

in 27 BC [3, 4]. This design was more common but less efficient than the overshot waterwheel until the 13th century [2], though the undershot type continued to be popular thereafter, for reasons we shall discuss below. In the 19th century it was made much more efficient, as we shall see, because of a development in France that anticipated the successor of waterwheel technology: hydraulic turbines.

It is hard to overstate the historical importance of waterwheels. They were the primary source of power from antiquity until the introduction of reliable high-pressure steam engines at the end of the 18th century [4] and their development over the millennium from 500 AD to 1500 AD represents the outstanding technological development of this period [2]. Early waterwheels (such as the 16 overshot wheels that formed the large Roman mill of 300 AD at Barbégal, near Arles, France, and generated perhaps 20 kW [5]) were geared down, so that the millstones turned more slowly than the waterwheels. This changed as designs improved over the centuries; by the Middle Ages mills were geared up as much as 5:2 [4]. It is widely considered [2, 3, 6] that the most dramatic industrial consequences of waterwheels occurred in the Middle Ages, when the scale of milling increased considerably with the development of large towns. Their considerable economic and social impact may be judged by the increased application of waterwheels [3, 7, 8]. From grinding grain and pumping water in antiquity, water powered mills were developed to forge iron, full cloth, saw wood and stone, and for metalworking and leather tanning. Later, waterwheels were applied to drive the machines of the early industrial revolution.

The power of waterwheels increased by a factor of three during the 18th century, to perhaps 10 kW. Much effort went into the scientific investigation of their efficiency. In 1704 Antoine Parent calculated the maximum efficiency of an idealized undershot waterwheel. In England John Smeaton (founder of the society of Civil Engineers) made scale models of both undershot and overshot waterwheel designs, during 1752–4. He varied components to establish empirically the most effective designs, and concluded that undershot were no more than 22% efficient whereas overshot were 63% efficient [2, 9]. In 1780 Leonhard Euler studied the latest waterwheel developments. In the early 19th century the French engineer J V Poncelet increased the power of undershot waterwheels, as we shall see, to that of overshot wheels [2, 6]. The famous 1835 paper of Coriolis was written, not on the subject of earth rotation, but rather on energy transfer in rotating systems such as waterwheels [10].

In this paper we shall develop simple models of the two main types of vertical waterwheel, overshot and undershot, which will bring to light the important technical issues and permit a realistic calculation of waterwheel efficiency. We shall see why overshot wheels are more efficient, why undershot continued to be used despite this, and why the modifications introduced by Poncelet were able to increase drastically undershot waterwheel efficiency. Our overshot waterwheel model of section 3 is quite general, and shows that waterwheels are stable dynamical systems even under rapidly changing load. Both overshot and undershot models are simple, yet illustrate which of the design parameters are important.

2. Idealized waterwheel

We begin with an idealized overshot waterwheel model, which will serve to introduce notation and some basic concepts. Consider figure 1. Here 12 triangular buckets are attached to the rim of a wheel. Each bucket is free to swivel about a horizontal axis. The buckets are filled with water, which here is assumed to drop vertically from a flume. The filled buckets cause the waterwheel to rotate. At a ‘spill angle’ θ_1 near the rim of the wheel is a baffle that causes the buckets to shed water—no water is spilled otherwise. We assume that the wheel is frictionless, and does work turning a millstone. The effect of the millstone is represented by a constant load torque G_L . We shall determine the equation of motion for this waterwheel, and shall estimate its efficiency.

The wheel has been constructed so that torque is applied solely from the gravitational potential energy of the water, and not from its momentum. The more realistic model in what

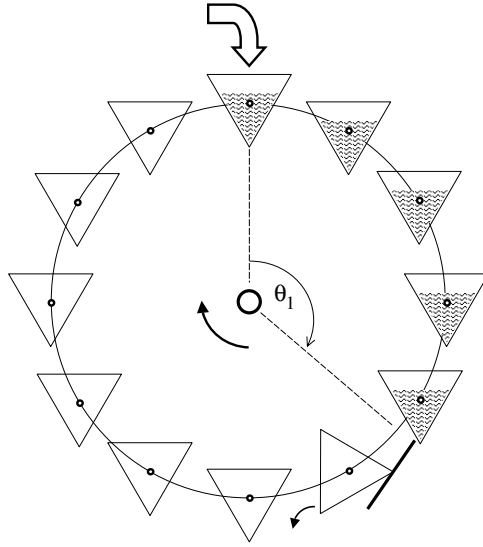


Figure 1. Idealized overshot waterwheel powered by gravitational potential energy (water head). Water drops vertically into buckets, and remains there until tipped out at angle θ_1 .

follows will include water momentum, as well as permit water spillage and allow for friction, and other such unavoidable realities. Here we can assume that those buckets at angle θ , where $0 < \theta \leq \theta_1$, are filled with water and that all the others are empty. There are n buckets each occupying an angle $\Delta\theta$ around the rim, so that $n \Delta\theta = 2\pi$. The mass of water in each bucket is $\Delta m = \rho f \Delta t$, where ρ is the water density (kg m^{-3}), f is the flow rate ($\text{m}^3 \text{s}^{-1}$) and Δt is the time interval over which water fills the bucket. We can obtain this from $\omega \Delta t = \Delta\theta$, where ω is waterwheel angular speed, so that

$$\Delta m = \frac{\rho f}{\omega} \Delta\theta. \quad (1)$$

Let us ignore the possibility of water overflowing, due to slow rotation rate, or due to fast rotation (centrifugal force). The torque applied about the waterwheel axle by the weight of water is $\Delta G = \Delta m g R \sin(\theta)$ per bucket, where R is the wheel radius and θ is the location of the filled bucket. For large n we can calculate the total torque as follows:

$$G \approx \frac{\rho g f R}{\omega} \int_0^{\theta_1} d\theta \sin(\theta) = \frac{\rho g f R}{\omega} [1 - \cos(\theta_1)]. \quad (2)$$

Again assuming that n is large, we shall ignore the torque (opposing that of equation (2)) arising from the buckets being emptied when they reach θ_1 . For this idealized waterwheel the equation of motion is

$$I \dot{\omega} = G - G_L \quad (3)$$

where I is the moment of inertia of the wheel plus water, and where $\dot{\omega} = d\omega/dt$. We shall not solve (3), but simply note that there is a stable state for this system with angular speed

$$\varpi = \frac{\rho g f R}{G_L} [1 - \cos(\theta_1)] \quad (4)$$

as is readily seen from (2) and (3).

We can calculate the efficiency of this waterwheel as follows. The energy input by each bucketful of water is $\Delta E_{\text{in}} = 2\Delta m g R$ and the corresponding power is $\Delta P_{\text{in}} = \Delta E_{\text{in}} \frac{\varpi}{\theta_1}$

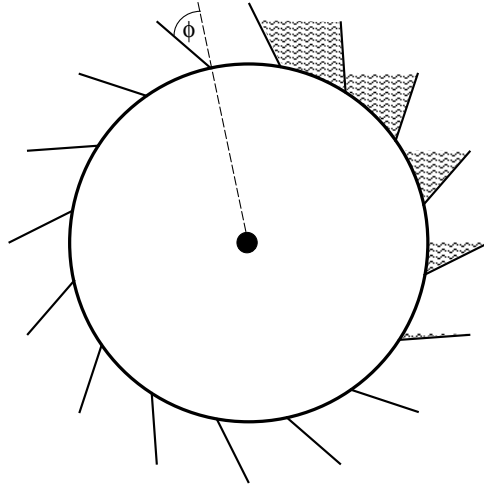


Figure 2. Overshot waterwheel with canted vanes (bucket separators). As the cant angle ϕ increases, water is retained for longer, increasing torque.

assuming that the wheel rotates at the constant steady-state rate $\bar{\omega}$. The total input power is $P_{\text{in}} = \frac{\theta_1}{2\pi} n \Delta P_{\text{in}} = 2\rho g f R$. Useful output power is $P_{\text{out}} = \bar{\omega} G_L$ and so waterwheel efficiency is found to be

$$\varepsilon \equiv \frac{P_{\text{out}}}{P_{\text{in}}} = \sin^2\left(\frac{1}{2}\theta_1\right). \quad (5)$$

So the efficiency of this idealized waterwheel is independent of all the parameters except the spill angle. This is a consequence partly of our idealizations and partly of our assumption that the wheel is powered solely by gravity, i.e. by the weight of water alone, and not its momentum. Efficiency can be 100% if the spill angle is $\theta_1 = \pi$, so that the water contributes to torque until it is at the bottom of the wheel. For practical waterwheels to which we now turn, this is difficult to achieve, so efficiency is reduced.

3. General overshot waterwheel efficiency

To make the overshot waterwheel model more realistic, we must make a number of changes. Firstly, real waterwheels did not have pivoted buckets—this device was adopted above to ensure that water did not spill out as the wheel turned. Instead, the rim of the wheel is partitioned off into sections, as suggested in figure 2. These rotate with the wheel, and so water spills out increasingly as θ increases. Also, water splashes over the sides as it flows in to the buckets, and flows from one bucket to lower buckets as the wheel turns. To allow for these effects, we assign a *loss factor* $x(\theta)$ to the buckets, describing the fraction of water that remains in the bucket. Thus $x(0) = 1$ and $x(\pi) = 0$; for other values of θ the loss factor takes on values that depend upon waterwheel design.

Water also may be lost due to centrifugal force. If the bucket walls are along radial lines ($\phi = 0$, in the notation of figure 2) then water is shed from the wheel for angles exceeding θ_{max} , for which the centripetal part of the gravitational force exceeds the centrifugal force. This leads to

$$\cos(\theta_{\text{max}}) = \frac{\omega^2}{\omega_{\text{max}}^2}, \quad \omega_{\text{max}}^2 \equiv \frac{g}{R}. \quad (6)$$

The total mass of water in the buckets, at any given instant, can be found from the foregoing to be

$$m = \frac{\rho f}{\omega} \int_0^{\theta_{\max}} d\theta x(\theta) \equiv \frac{\rho f}{\omega} X_0(\omega) \quad (7)$$

where the integrated loss factor X_0 depends upon ω through equation (6). Similarly, from a calculation analogous to that of the last section, the total torque due to gravity is

$$G_g = \frac{\rho g f R}{\omega} \int_0^{\theta_{\max}} d\theta x(\theta) \sin(\theta) \equiv \frac{\rho g f R}{\omega} X_1(\omega). \quad (8)$$

There is an additional driving torque G_w , due to the momentum of the water from the *headrace* (the flume leading to the waterwheel), determined as follows. The force of water striking the vanes on the waterwheel rim is $F = \rho f(v - \omega R)$, i.e. the mass per second of water striking the vanes, multiplied by the change in speed of the water as a consequence of striking the vanes [11]. Here v is the component of water speed that is tangential to the wheel, and ωR is the speed of the vanes. The torque is thus

$$G_w = \rho f R(v - \omega R). \quad (9)$$

The equation of motion is (see equation (3)) $I\dot{\omega} = G_g + G_w - G_L - G_k$. Here we have allowed for kinetic friction, for example at the waterwheel axle, generating a torque G_k , assumed constant. Substituting from equations (7)–(9):

$$\left(\eta M R^2 + \frac{\rho f}{\omega} X_0(\omega) R^2 \right) \dot{\omega} = \frac{\rho g f R}{\omega} X_1(\omega) + \rho f R(v - \omega R) - G_L - G_k. \quad (10)$$

The wheel has mass M and moment of inertia $\eta M R^2$, where $\frac{1}{2} < \eta < 1$; the precise value of η depends upon waterwheel structure. Again, G_L is the torque due to the load. Equation (10) is valid for low values of water speed v and low angular speed ω . For higher values of v we might expect the water to be less effective than suggested in (9) at imparting torque to the waterwheel², while for higher ω we should include a speed-dependent air resistance term. As a practical limit upon the validity of (10), we note that if v is large enough so that $G_w = G_L + G_k$ then the steady-state angular speed is $\bar{\omega} = \omega_{\max}$. For larger v there is no steady state. Instead, angular speed is always increasing. Yet it is observed that, even in the absence of load, a waterwheel does not accelerate indefinitely. Thus, we consider that (10) is valid if $G_w \leq G_k$; for larger values of v we must include other energy-dissipating terms in (10).

The steady-state angular speed $\bar{\omega}$, found by setting the right-hand side of equation (10) to zero, is the solution to

$$G_L + G_k - \rho f R(v - \bar{\omega} R) \approx \frac{\rho g f R}{\bar{\omega}} X_1(\bar{\omega}). \quad (11)$$

We expect (see what follows) $\bar{\omega} \ll \omega_{\max}$ and so we can solve (11) iteratively:

$$\bar{\omega}^{(0)} = \frac{\rho g f R X_1(0)}{G_L + G_k - \rho f R v}, \quad \bar{\omega}^{(1)} = \frac{\rho g f R X_1(\bar{\omega}^{(0)})}{G_L + G_k - \rho f R(v - \bar{\omega}^{(0)} R)}, \dots \quad (12)$$

We can see by inspection of (10) that this state is stable: if $\omega = \bar{\omega} + \delta$ then $\text{sign}(\dot{\omega}) = -\text{sign}(\delta)$. Thus, any perturbation away from $\bar{\omega}$ causes angular speed to revert to $\bar{\omega}$.

In figure 3 we show the result of numerically integrating equation (10) for two cases (see table 1), differing in the form assumed for the loss factor $x(\theta)$ of equations (7) and (8).

This confirms that the steady-state angular speed is stable. For the numerical integration we have recast equation (10) in terms of dimensionless variables

$$\frac{ds}{d\tau} = \frac{X_1(s) - \frac{s}{\bar{s}} X_1(\bar{s}) - s(s - \bar{s})}{C s + X_0(s)}, \quad s \equiv \frac{\omega}{\omega_{\max}}, \quad \tau = \omega_{\max} t, \quad (13)$$

$$\bar{s} \equiv \frac{\bar{\omega}}{\omega_{\max}}, \quad C \equiv \frac{\eta M \omega_{\max}}{\rho f}.$$

² Water that has just struck a vane may be unable to ‘get out of the way’ of water that is about to strike the vane. So, some of the high-speed water momentum is dissipated before being imparted to the vane.

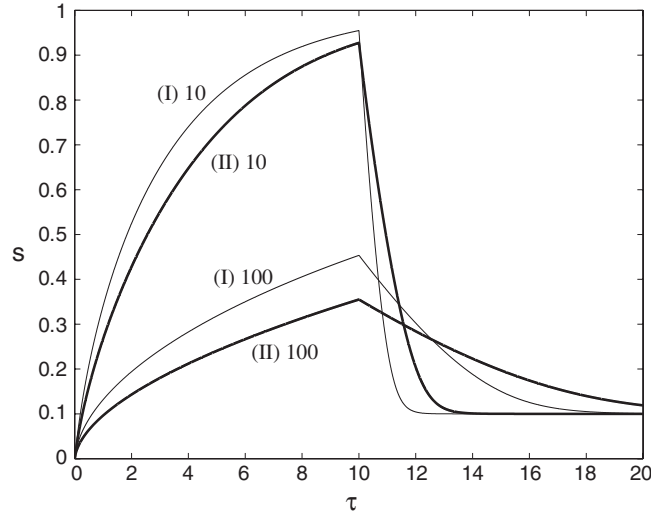


Figure 3. Dimensionless angular speed s versus dimensionless time τ for the overshoot waterwheel model of equation (13). The dimensionless steady-state angular speed \bar{s} is set equal to 1 in the absence of load, and is set to 0.1 when a load is applied at $\tau = 10$ (see equation (12)). The waterwheel quickly adjusts to the new load, for cases (I) and (II) of table 1, and for parameter values $C = 10$ and 100. The waterwheel operates more efficiently with a large load than with a small one. See section 4 for details.

Table 1. Two loss factors $x(\theta)$ considered in the text, and the corresponding integrated loss factors $X_{0,1}$.

	$x(\theta)$	$X_0(\omega)$	$X_1(\omega)$
Case I	1	$\cos^{-1}\left(\frac{\omega^2}{\omega_{\max}^2}\right)$	$1 - \frac{\omega^2}{\omega_{\max}^2}$
Case II	$\cos(\theta)$	$\sqrt{1 - \frac{\omega^4}{\omega_{\max}^4}}$	$\frac{1}{2}\left(1 - \frac{\omega^4}{\omega_{\max}^4}\right)$

There are thus two parameters in this model, C and \bar{s} .

We can obtain a general expression for the dependence of $\bar{\omega}$ upon water speed v , by differentiating equation (11) with respect to v . If the load G_L and frictional torque G_k are independent of v then this yields

$$\frac{d\bar{\omega}}{dv} = \frac{1}{R} \left[1 + 2x(\bar{\theta}_{\max}) + \frac{X_1(\bar{\omega})}{\cos(\bar{\theta}_{\max})} \right]^{-1}, \quad \bar{\theta}_{\max} = \cos^{-1}\left(\frac{\bar{\omega}^2 R}{g}\right). \quad (14)$$

In deriving (14) we have made use of equations (6) and (8). Equation (14) shows that, whatever the form of the loss factor $x(\theta)$, the steady-state angular speed *increases* with water speed. Similarly we can show that $\bar{\omega}$ *decreases* as wheel radius R increases.

Now we are in a position to calculate the overshoot waterwheel efficiency. Compared to the idealized case we find that the input power changes from $P_{\text{in}} = 2\rho g f R$ to $2\rho g f R + \frac{1}{2}\rho f v^2$; the extra term is the power of the flowing water [11]. Output power is $P_{\text{out}} = \bar{\omega} G_L$ as before, and so waterwheel efficiency is

$$\varepsilon = \frac{X_1(\bar{\omega})}{2 + \frac{v^2}{2gR}} \frac{G_L}{G'_L}. \quad (15)$$

The derivation of (15) is valid only if $G_w \leq G_k$, and so we require $G_L \leq G'_L$. Let us say for simplicity that water speed v from the headrace has been chosen so that the torque imparted by water momentum transfer exactly balances friction at the axle: $G_w = G_k$ and so $G_L = G'_L$. From (15) we see that, from the form of the integrated loss factor $X_1(\bar{\omega})$, efficiency decreases as steady-state angular speed increases. Also efficiency falls as water speed v increases ($X_1(\bar{\omega})$ decreases as $\bar{\omega}$ increases and so, from (14), as v increases). From a similar argument we see that efficiency is increased as wheel radius R increases. So efficient design calls for low v , low $\bar{\omega}$ and large R : this accords with experience and observation of real waterwheels. Thus we conclude that the simple model developed here captures significant features of overshot waterwheel physics.

If the vane angle ϕ of figure 2 is greater than zero, then water is shed from the wheel for angles exceeding θ_{\max} , where

$$\cos(\theta_{\max} - \phi) = \omega^2 \frac{R}{g} \cos(\phi) \quad (16)$$

(see equation (6)). Repeating the development above for nonzero ϕ leads to, assuming Case I for $X_1(\bar{\omega})$ (more precisely, a design with $X_1(\bar{\omega}) \rightarrow 1$ as $\bar{\omega} \rightarrow 0$) and small $\bar{\omega}$

$$\varepsilon = \frac{1 + \sin(\phi)}{2 + \frac{v^2}{2gR}} \quad (17)$$

so efficiency is increased if $\phi > 0$. Again, this appears to be the case in practice, since most overshot waterwheels have buckets which are canted in this way, with the partitions between buckets (the vanes) as shown in figure 2. If we adopt the reasonable parameter values $\phi = 30^\circ$, $v = 2 \text{ m s}^{-1}$, and $R = 2 \text{ m}$ then $\varepsilon = 71\%$, which is close to Smeaton's figure of 63%. From (15) and (17) we see that the parameters that most influence overshot waterwheel efficiency are (assuming small $\bar{\omega}$) ϕ and $X_1(0)$.

4. Undershot waterwheel efficiency

Here we present a simple model of undershot waterwheels from which we calculate their efficiency, and show why Poncelet's modification improved things significantly. Before doing so, it is appropriate here to discuss the reason why this mattered so much. Given the threefold superiority of overshot efficiency, why persist with undershot waterwheels at all? To understand this, we must appreciate the ubiquity of waterwheels in Europe, at the beginning of the industrial revolution, prior to the widespread availability of steam engines. We have already stressed the importance of waterwheels since antiquity, as a source of power. The Domesday Book of 1086 recorded over 5000 mills in England. By 1820 France alone had 60 000 waterwheels. The dense population of mills along early 19th century European rivers and streams meant few hydro sites, so water *head* (height difference, and thus potential energy) became a scarce and valuable resource. Overshot wheels required a large head (2–10 m) and so were usually confined to hilly areas, or required extensive and expensive auxiliary construction, such as mill races (water flumes or sluices) that ran for hundreds of metres. Undershot wheels, on the other hand, could operate with less than 2 m head and so could be located on small streams in flat areas, nears to population centres. Thus they remained important well beyond the period when scientific investigation had shown them to be relatively inefficient. The French government offered large prizes for improved waterwheel design, and this spurred a lot of theoretical and experimental investigations. Poncelet won a prize with his modified waterwheel vanes, which proved to be an immediate success.

Conventional undershot design

To estimate the efficiency of undershot waterwheels, consider figure 4(a). We shall simplify the analysis by assuming that wheel radius is large, so that the water flow is normal to the

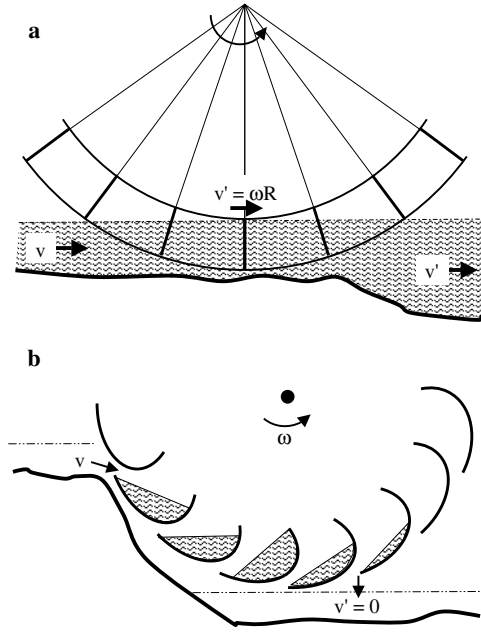


Figure 4. (a) Undershot waterwheel with radial vanes. The water flow approaching (receding from) the wheel has mean speed v (v'). The wheel rotates at constant angular speed $\bar{\omega} = v'/R$. (b) Poncelet's modification: curved vanes that trap the water, releasing it only when the water has transferred most of its horizontal momentum. Achieving this requires a careful balancing of vane shape and water flow rate.

vanes. Thus, if the vane area is A , then the mass of water that presses against each vane per unit time is $\dot{m} = \rho A(v - v')$. Here v is mean water speed before transferring momentum to the waterwheel, and $v' = \omega R \equiv cv$ is the mean water speed afterwards, both assumed constant. Thus we expect $0 < c < 1$. The force exerted by the water against the vanes is $F = \frac{d}{dt}(m(v - v')) = \rho Av^2(1 - c)^2$. The output power of the waterwheel, resulting from this force, is $P_{\text{out}} = Fv'$; this is the applied force multiplied by the distance moved by the vanes per unit time [11]. Thus $P_{\text{out}} = \rho Av^3 c(1 - c)^2$.

The input energy is $dE_{\text{in}} = \frac{1}{2}\rho Av^2 dx$ for a water lamina of width dx . So the input power is $P_{\text{in}} = \frac{1}{2}\rho Av^3$, since $\frac{d}{dt}x = v$. Thus, the waterwheel efficiency is

$$\varepsilon = \frac{P_{\text{out}}}{P_{\text{in}}} = 2c(1 - c)^2. \quad (18)$$

This peaks for $c = \frac{1}{3}$ (so that the waterwheel vanes move at a third of the initial water speed in the millrace) so that the maximum efficiency of the undershot waterwheel is about 30%. Given the simplicity of our analysis, this is remarkably close to Smeaton's figure of 22%. We have not allowed for loss of energy (due, for example, to water splashing) or for the finite wheel radius, both of which would reduce our estimate. The equation of motion for the undershot waterwheel is $I\dot{\omega} = G_w - G_L - G_k$ where the torque due to water flow is $G_w = FR = \rho AR(v - \omega R)^2$. A steady-state angular speed $\bar{\omega}$ is found by setting $\dot{\omega} = 0$, as before; if the waterwheel design is such that $\bar{\omega}R = \frac{1}{3}v$ then this is the most efficient operating speed. For such a design the load can be expressed in terms of other parameters:

$$G_L = \frac{4}{9}\rho ARv^2 - G_k. \quad (19)$$

Thus water speed is the most important factor in determining maximum load, for undershot waterwheels.

Poncelet modification

This consisted of a careful reshaping of the vanes, as shown in figure 4(b). These curved vanes hold the water as the wheel rotates; the water falls back (off the outside edge of the vane) with zero speed, $v' \approx 0$, if the vane is properly adjusted to the water speed. Thus efficiency is improved for two reasons. Firstly, a gravitational component of torque is provided, as with overshot wheels. Secondly, more of the mill race water momentum is transferred to the wheel. We can account for this latter effect as follows. The analysis is as for conventional undershot design except that now the force exerted by water pressing against the vanes is given by $F = \rho A v^2 (1 - c)$, since here the speed difference of the water, resulting from interaction with the vane, is approximately v , and not $v - v'$. Calculating input and output powers as before leads to the following expression for Poncelet waterwheel efficiency:

$$\varepsilon = 2c(1 - c) \quad (20)$$

(see equation (18)). We expect that this is an underestimate, since our simple analysis does not allow for the extra gravitational contribution to torque. From (20) we see that efficiency peaks for $c = 1/2$ at $\varepsilon = 50\%$. This is a significant improvement. The efficiencies obtained by Poncelet were higher than this (about 65%); we attribute the difference to gravitational torque, as described above. The combination of undershot design with some gravitational power input is known as a *breast shot* waterwheel, and is a 19th century invention, combining elements of overshot and undershot designs. The most efficient of these is the Poncelet type. From figure 4(b) we see that the curved vanes anticipate the shape of hydraulic turbines.

5. Summary and discussion

For pedagogical purposes we have been able to model waterwheel physics by using only elementary concepts (force, torque, energy, power) from mechanics and fluid dynamics.

The simple overshot and undershot waterwheel models developed here can account quite well for the measured efficiencies. The undershot model explains why the Poncelet modification significantly improved efficiency. Both models highlight those parameters that are important in waterwheel design. For example, it is not difficult to derive the following expression for the ratio of undershot to overshot power output

$$\frac{P_{\text{us}}}{P_{\text{os}}} \approx \frac{8}{27} \frac{v^2}{gR(1 + \sin(\phi))}. \quad (21)$$

(Here we have made a number of assumptions. The undershot wheel is optimum, and the overshot wheel has $X_1(\bar{\omega}) \approx 1$ and low friction.) For realistic parameter values this shows that the overshot wheel is significantly more powerful, particularly for low flow rate and large wheel radius.

Acknowledgments

The author is grateful to JSTOR library services of U Michigan for providing the full reference [9] for Smeaton's paper. This paper '*An Experimental Enquiry concerning the Natural Powers of Wind and Water to Turn Mills, and Other Machines, Depending on a Circular Motion*' was originally delivered to the Royal Society in May 1759.

References

- [1] Strogatz S H 1994 *Nonlinear Dynamics and Chaos* (Reading, MA: Addison-Wesley) pp 301–11
- [2] Waterwheels *Encyclopaedia Britannica* CD 98
- [3] Usher A P 1988 *A History of Mechanical Inventions* (New York: Dover) chapter 7
- [4] Landels J G 1978 *Engineering in the Ancient World* (London: Constable) chapter 1

-
- [5] James P and Thorpe N 1994 *Ancient Inventions* (New York: Ballantine) chapter 9
 - [6] Mason S F 1962 *A History of the Sciences* (New York: Macmillan) pp 74, 105, 276
 - [7] Gies F and Gies J 1995 *Cathedral, Forge, and Waterwheel: Technology and Invention in the Middle Ages* (New York: Harper Collins)
 - [8] *Hutchinson Encyclopedia* 1998 (Godalming, UK: Helicon) pp 1131–2
 - [9] Smeaton J 1759 *Phil. Trans. R. Soc.* **51** 100–74
 - [10] Coriolis G G J 1835 *Ec. Polytech.* **15** 142–4
 - [11] Douglas J F and Matthews R D 1996 *Fluid Mechanics* (Harlow, UK: Longman) chapter 8